

# 3D MHD simulation of polarized emission in SN 1006

E. M. Schneider<sup>1,2,3\*</sup>, P. F. Velázquez<sup>4</sup>, E. M. Reynoso<sup>5,6</sup>, A. Esquivel<sup>4</sup>,  
F. De Colle<sup>4</sup>

<sup>1</sup>*Instituto de Astronomía Teórica y Experimental, Universidad Nacional de Córdoba, Córdoba, Argentina*

<sup>2</sup>*Departamento de Materiales y Tecnología, UNC, Córdoba, Argentina*

<sup>3</sup>*Department of Astronomy & Oskar Klein Centre, Albanova, Stockholm University, SE-106 91 Stockholm, Sweden*

<sup>4</sup>*Instituto de Ciencias Nucleares, Universidad Nacional de México, México D. F. México*

<sup>5</sup>*Instituto de Astronomía y Física del Espacio, Suc. 28, CP: 1428, Buenos Aires, Argentina*

<sup>6</sup>*Physics Department, Faculty of Exact and Natural Sciences, University of Buenos Aires, Argentina*

Accepted . Received

## ABSTRACT

We use three dimensional magnetohydrodynamic (MHD) simulations to model the supernova remnant SN 1006. From our numerical results, we have carried out a polarization study, obtaining synthetic maps of the polarized intensity, the Stokes parameter  $Q$ , and the polar-referenced angle, which can be compared with observational results. Synthetic maps were computed considering two possible particle acceleration mechanisms: quasi-parallel and quasi-perpendicular. The comparison of synthetic maps of the Stokes parameter  $Q$  maps with observations proves to be a valuable tool to discern unambiguously which mechanism is taking place in the remnant of SN 1006, giving strong support to the quasi-parallel model.

**Key words:** MHD–radiation mechanisms: general – methods : numerical – supernovae: individual: SN 1006 –ISM: supernova remnants

## 1 INTRODUCTION

Recently, the study of bilateral (also known as barrel-like) supernova remnants (SNR) has gained great interest since they have proven to be a useful tool when studying the configuration of the interstellar magnetic field (ISMF) on scales of a few pc. As their name suggests, these type of SNRs display two characteristic bright and opposite arcs. The morphology of this type of remnants has been explained with an ISMF, which is involved in the acceleration mechanism of relativistic particles. However, there is still debate as to which is the most efficient acceleration mechanism in these objects. One interpretation is the equatorial belt model, in which the orientation of the ISMF is quasi-perpendicular to the shock front normal. The other interpretation is the polar cap model in which they are quasi-parallel.

The remnant of SN 1006 is the archetype of the bilateral SNR group. It has a diameter of  $30'$  (or 20 pc at a distance of 2.2 kpc, Winkler et al. 2003) and, in radio-continuum and X-ray images, exhibits an incomplete shell with two bright arcs perpendicular to the Galactic plane (Reynolds & Gilmore 1993; Reynoso et al. 2013). SN 1006 is accepted to be the result of a type Ia SN explosion (Stephenson & Green 2002). This remnant is located at a high Galactic lat-

itude, and therefore thought to be evolving in an almost homogeneous interstellar medium (ISM). For this reason, the radio-continuum morphology of the remnant must be mostly affected by the characteristics of the surrounding ISMF.

Numerous theoretical and observational studies have been devoted to analyze which mechanism is responsible for the morphology of this remnant, giving rise to two opposing interpretations: either the quasi-perpendicular acceleration mechanism (e.g. Fulbright & Reynolds 1990; Petruk et al. 2009; Schneider et al. 2010) or the quasi-parallel mechanism (e.g. Völk et al. 2003; Rothenflug et al. 2004; Bocchino et al. 2011).

Most of these works apply criteria based only on the brightness distribution of the synchrotron emission. Accordingly, their conclusions are strongly dependent on the orientation of the ISMF respect to the line of sight ( $los$ ), and can not determine which particle acceleration mechanism is actually taking place. A recent observational polarization study seems to favour the idea that the bright arcs of SN 1006 can be explained by the polar cap model, implying an ISMF parallel to the Galactic plane (Reynoso et al. 2013).

The present work is an effort to clarify which process or mechanism is more suitable to explain the synchrotron emission of the remnant of SN 1006. For this purpose, we carried out 3D MHD simulations employing the same scenario pro-

\* Email: mschneider@gmail.com

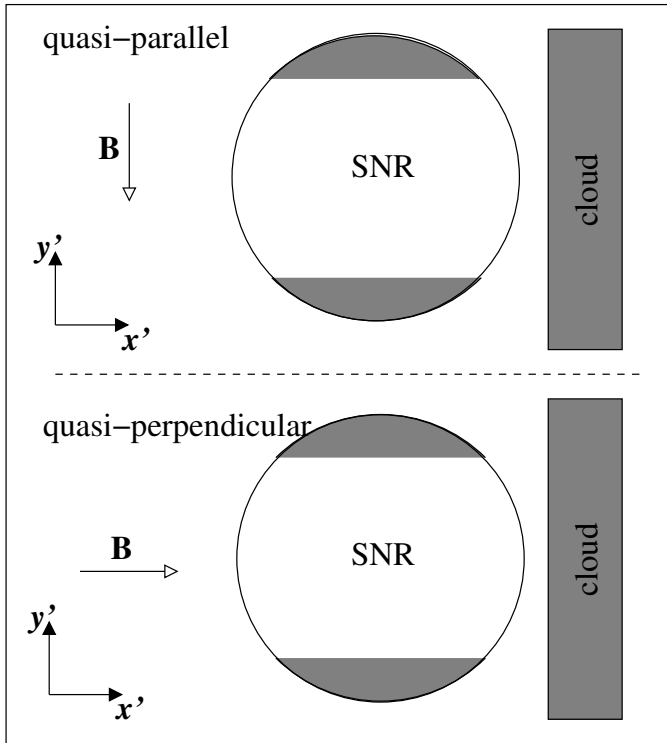


**Figure 1.** Scheme of the numerical setup employed in our simulations for the quasi-parallel (top panel) and the quasi-perpendicular case (bottom panel). In all the models a dense cloud was placed to the right.

posed in Schneider et al. (2010). From the numerical results, we performed a polarization analysis of the Stokes parameters  $Q$  and  $U$ , as well as the polar-referenced angle, thus facilitating the direct comparison with observations.

The organization of this work is as follows: section §2 presents the initial setup for the MHD simulations, section §3 explains how the synthetic maps for the radio emission and Stokes  $Q$  and  $U$  parameters were calculated, section §4 introduces the results obtained which are further discussed and summarized in section §5.

## 2 THE NUMERICAL MODEL

### 2.1 Initial setup

The numerical simulations were carried out with the parallelized 3D MHD code Mezcald (De Colle & Raga 2006; De Colle et al. 2008, 2012). This code solves the full set of ideal MHD equations in cartesian geometry  $(x', y', z')$  with an adaptive mesh, and includes a cooling function to account for radiative losses (De Colle & Raga 2006). The computational domain is a cube of 24 pc per side and it is discretized on a six level binary grid, with a maximum resolution of  $2.3 \times 10^{-2}$  pc. All the outer boundaries were set to an out-flow condition (gradient free).

### The SNR

The physical parameters of the SNR setup are the same as those presented in Schneider et al. (2010), but to help the readability of the present paper, we reproduce them below.

A supernovae explosion is initialized by the deposition of  $E_o = 2.05 \times 10^{51}$  erg of energy in a radius of  $R_o = 0.65$  pc located at the centre of the computational domain. The energy is distributed such that 95% of it is kinetic and the remaining 5% is thermal.

The ejected mass was distributed in two parts: an inner homogeneous sphere of radius  $r_c$  containing 4/7ths of the total mass ( $M_* = 1.4M_\odot$ ) with a density  $\rho_c$ , and an outer shell containing the remaining 3/7ths of the mass following a power law ( $\rho \propto r^{-7}$ ) as in Jun & Norman (1996b). The velocity has a linear profile with  $r$ , which reaches a value of  $v_o$  at  $r = R_o$ . The parameters  $\rho_c$ ,  $r_c$ , and  $v_o$  are functions of  $E_o$ ,  $M_*$ , and  $R_o$ , and were computed using Eqs.(1)-(3) of Jun & Norman (1996b).

### The surrounding interstellar medium

The surrounding ISM, where the SNR evolves, was simulated as an homogeneous plasma with temperature  $T_o = 10^4$ K and number density  $n_o = 5 \times 10^{-2} \text{cm}^{-3}$ . At a distance of  $\sim 8$ pc in the  $x'$ -direction from the centre of the computational domain, the density was increased by a factor of 3 (Acero et al. 2007). The SNR will collide with this ‘wall’, producing a bright H $\alpha$  emission filament (Winkler et al. 2003), which has X-ray and radio counterparts (Acero et al. 2007; Schneider et al. 2010).

In order to simulate the synchrotron emission of SN 1006, based on the results of Schneider et al. (2010) we have considered two configurations for the magnetic field  $\mathbf{B}$  depending on which of the particle acceleration processes is assumed. For the quasi-perpendicular case,  $\mathbf{B}$  is along the  $x'$ -direction, and it is along the  $y'$ -direction for the quasi-parallel case (the bright arcs are in the  $y'$ -direction). In both cases, we have considered a mean magnetic field magnitude of  $2\mu\text{G}$ , while only for the quasi-parallel case an additional  $\nabla\mathbf{B}$ , increasing toward the  $-x'$ -direction, was included (which corresponds to model GRAD2 of Bocchino et al. 2011). Figure 1 shows a scheme of the initial numerical setup employed in our simulations.

## 3 SYNTHETIC TOTAL AND POLARIZED RADIO EMISSION MAPS

### 3.1 Synchrotron emission maps

The synchrotron emission is obtained as (Ginzburg & Syrovatskii 1965):

$$i(\nu) \propto K B_\perp^{\alpha+1} \nu^{-\alpha} \quad (1)$$

where  $\nu$  is the observed frequency,  $B_\perp$  is the component of the magnetic field perpendicular to the  $los$ , and  $\alpha$  is the spectral index which was set to 0.6 for this object. The coefficient  $K \propto \epsilon v_s^{-b}$  includes the dependence from the obliquity and the shock velocity  $v_s$  (Orlando et al. 2007), where  $\epsilon$  is either proportional to  $\sin^2 \Theta_{Bs}$  for the quasi-perpendicular case or  $\cos^2 \Theta_{Bs}$  for the quasi-parallel case. The angle  $\Theta_{Bs}$  is the angle between the shock normal and the post-shock

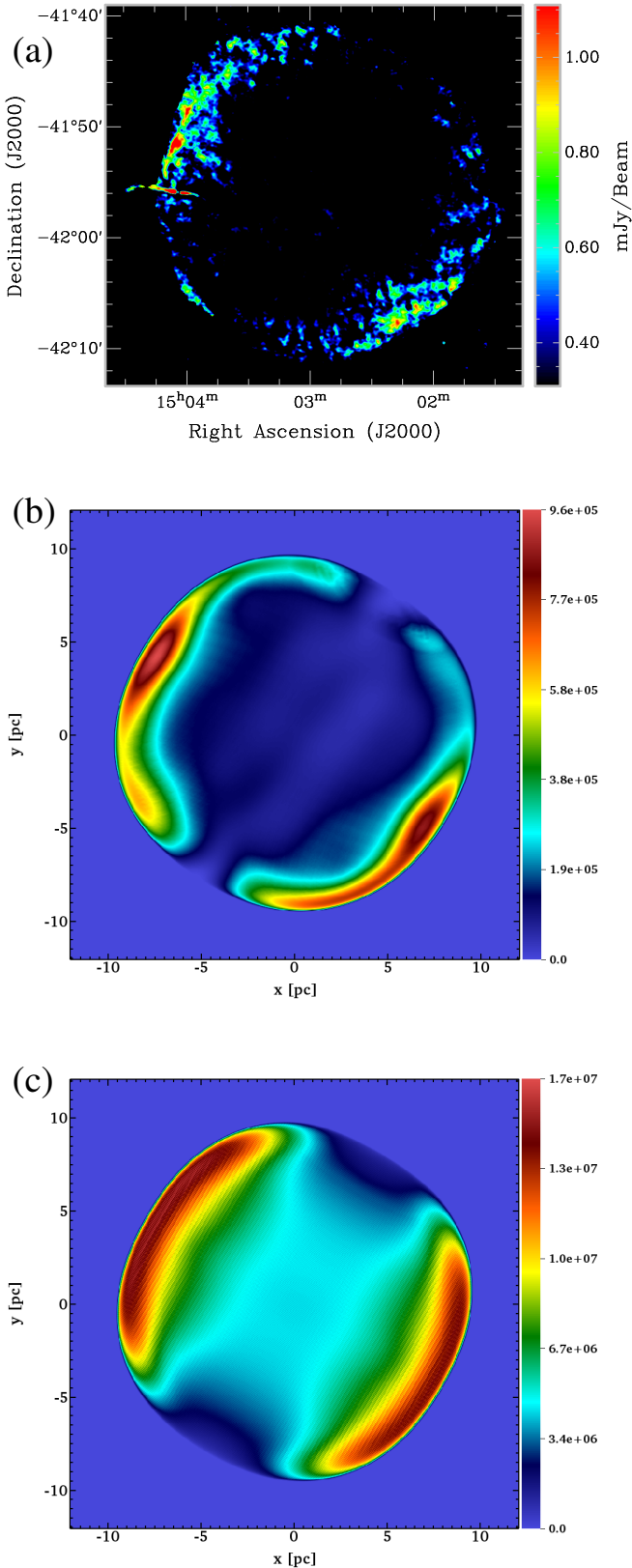


**Figure 2.** Synthetic maps of polarized intensity obtained for the quasi-parallel (panel b) and quasi-perpendicular (panel c) cases. The axes are in pc and the linear color scale is in arbitrary units. These maps were rotated 60 degrees with the purpose of comparing them to a radio image at 1.4 GHz (panel a), displayed in equatorial coordinates.

magnetic field (Fullbright & Reynolds 1990). As in Orlando et al. (2007), the exponent  $b$  was chosen to be  $-1.5$ , implying that stronger shocks are more efficient injecting particles.

### 3.2 Maps of the Stokes parameters

To calculate the  $Q$  and  $U$  synthetic maps, the following expressions for the Stokes parameters were employed (see Clarke et al. 1989; Jun & Norman 1996a)

$$Q(\nu) = \int_{los} f_0 i(\nu) \cos[2\phi(s)] ds \quad (2)$$

$$U(\nu) = \int_{los} f_0 i(\nu) \sin[2\phi(s)] ds \quad (3)$$

where  $s$  increases along the  $los$ ,  $\phi(s)$  is the position angle of the local magnetic field on the plane of the sky, and  $f_0$  is the degree of linear polarization, which is function of the spectral index  $\alpha$ :

$$f_0 = \frac{\alpha + 1}{\alpha + 5/3} \quad (4)$$

The linearly polarized intensity is given by:

$$I_P(\nu) = \sqrt{Q(\nu)^2 + U(\nu)^2} \quad (5)$$

and the polarization angle was computed as follows:

$$\chi = \frac{1}{2} \tan^{-1}(U/Q) \quad (6)$$

### 3.3 Observations

In order to compare our simulations with SN1006 as observed in radio wavelengths, we have made use of data obtained at 1.4 GHz with the Australia Telescope Compact Array (ATCA) and the Very Large Array (VLA), already published in Reynoso et al. (2013). These data contain information on the polarization of the emission, thus we constructed a map of the polarized intensity (Fig. 2a) and another map with the  $Q$  parameter (Fig. 3a). The observations and data reduction process are described in Reynoso et al. (2013). The images presented here are convolved with a beam of 15 arcsec. To remove spurious features beyond the limits of SN1006, only pixels where the total intensity is above  $75 \text{ mJy beam}^{-1}$  are retained.

## 4 RESULTS

### 4.1 Synthetic polarization maps

Synthetic polarized intensity maps were constructed from our numerical simulation results, using Eq.(5). Figure 2 displays a comparison of the observed polarized emission (panel a), and the synthetic maps for the quasi-parallel (or polar cap model, panel b) and quasi-perpendicular (or equatorial belt model, panel c) cases. Before integrating along the  $los$  the computational domain (the  $x'y'z'$ -system) was tilted  $60^\circ$  counterclockwise around the  $z$ -axis (the  $los$ ), such that the North points upwards and the East to the left (the plane of the sky is the  $xy$  plane). In addition, both models were rotated  $15^\circ$  around the  $y$ -axis. The quasi-parallel model was further rotated  $15^\circ$  in the  $x$ -axis. Both synthetic

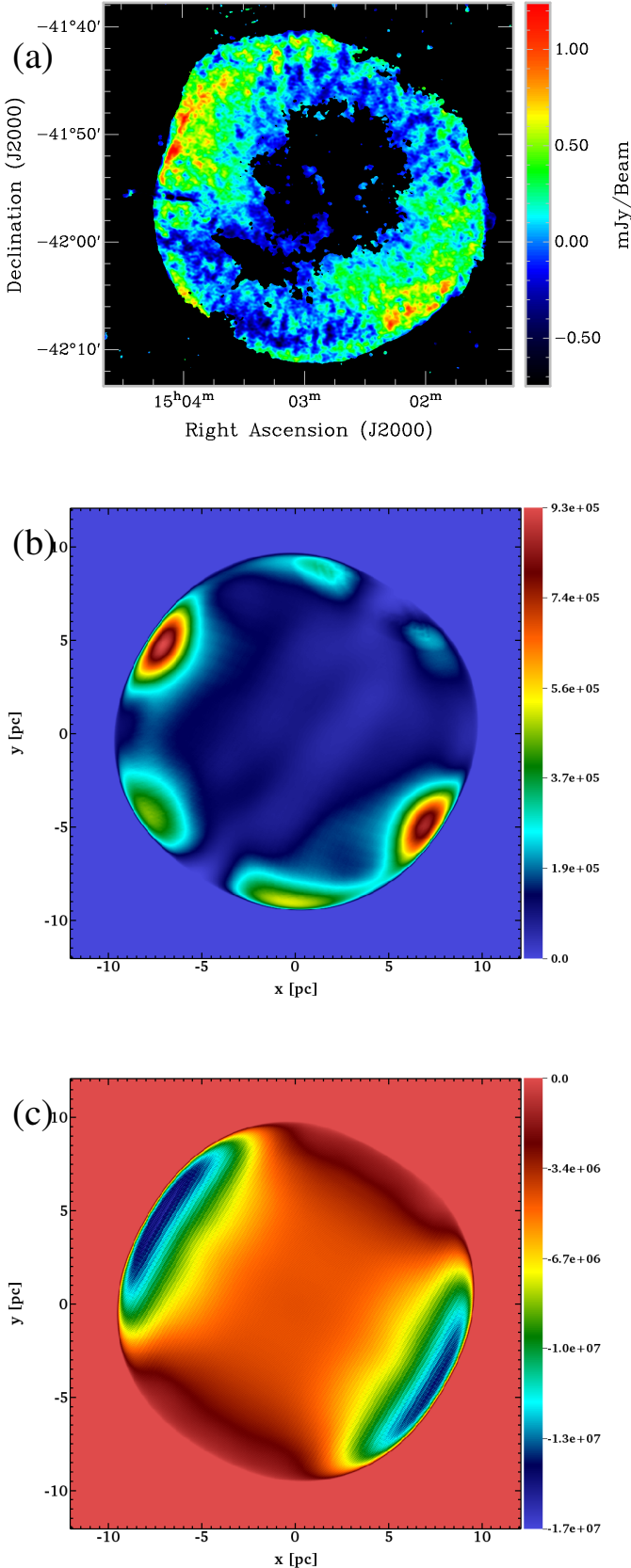


**Figure 3.** Comparison between the synthetic Stokes parameters  $Q$  for the quasi-parallel and the quasi-perpendicular cases (panels (b) and (c), respectively) with observations (panel a).

maps exhibit two bright arcs in the NE and SW direction, resembling the observations. The magnetic field gradient along the  $x$ -direction introduced in the simulations produces a SW-NE asymmetry in the polar cap model, in agreement with Bocchino et al. (2011) and with observations (see Reynoso et al. 2013, and Figure 2 in this paper). As expected, the equatorial belt model shows greater intensity due to a higher efficiency in diffusive shock acceleration (Jokipii 1987; Rothenflug et al. 2004; Cassam-Chenaï et al. 2008).

#### 4.2 Stokes parameter $Q$

In order to compare the simulated maps of the Stokes parameter  $Q$  with the observational one, we had to take into account that the observation of radio polarization from the SNR actually gives the position angle of the electric field. Hence, we had to follow the inverse process to the observational one, that is, the magnetic field was rotated clockwise  $90^\circ$ , emulating the perpendicular electric field, and then we performed the inverse Faraday correction. To clarify, we have replaced the argument  $\phi(s)$  in the trigonometric functions of Eqs. (2) and (3) by  $\phi(s) - \pi/2 + \Delta\chi_F$ , where  $\Delta\chi_F$  is the Faraday rotation correction, given by:

$$\Delta\chi_F = \frac{RM}{[\text{rad m}^{-2}]} \left( \frac{\lambda}{[\text{m}]} \right)^2 \quad (7)$$

being  $RM$  the rotation measure and  $\lambda$  the observed wavelength. For the case of the SN 1006, Reynoso et al. (2013) obtained an average  $RM$  of  $12 \text{ rad m}^{-2}$  from their polarization study at  $\lambda = 0.21 \text{ m}$ . With these values, Eq.(7) gives a correction angle due to Faraday rotation of  $0.52 \text{ rad}$  or  $30.3^\circ$ .

Figure 3 shows the resulting synthetic maps of the  $Q$  parameter (panels (b) and (c) for the quasi-parallel and the quasi-perpendicular cases, respectively), which were compared to the observed map (panel a).

As mentioned above, the question about which process of acceleration of relativistic particles is responsible for the synchrotron emission in SNRs (see Fulbright & Reynolds 1990; Petruk et al. 2009; Schneider et al. 2010; Völk et al. 2003; Rothenflug et al. 2004; Bocchino et al. 2011) is an ongoing discussion in the literature. Our simulated polarized intensity maps are not conclusive on which of the two competing processes better explains the case of SN 1006. However, the maps of the Stokes parameter  $Q$  are quite different between the two models, thus removing the discrepancy. Hence, the Stokes parameters turn out to be an important tool to compare numerical models with observations and determine which of the acceleration processes is more suitable in each scenario.

#### 4.3 Polar-referenced angles

Following Reynoso et al. (2013), we created maps of the angular difference for the position angle  $\chi$  with respect to the local radial direction  $\hat{r}$ , i.e. we obtained maps with the distribution of the polar-referenced angle  $\chi_r$ , which is given by:

$$\chi_r = \cos^{-1}(\hat{r} \cdot \hat{b}_\perp) \quad (8)$$

where  $\hat{b}_\perp$  is the direction of the magnetic field on the plane of the sky. In this representation,  $\chi_r = 0^\circ$  and  $\chi_r = \pm 90^\circ$  correspond to the radial and tangential directions respectively. These maps allow us to analyze two aspects of the magnetic field: the orientation of the post-shocked magnetic field and the orientation of the unshocked magnetic field of the ambient ISM. We expect the magnetic fields in young SNRs to be radially aligned due to the development of hydrostatic instabilities (Jun & Norman 1996a). So, the polar-referenced angle,  $\chi_r$ , should have a value close to zero on the edge of the shell.

Figure 4 shows maps of the distribution of  $\chi_r$ , obtained for both quasi-parallel and quasi-perpendicular cases. These maps show a very small region on the SNR periphery with radial magnetic field orientation, and  $\chi_r$  takes values that run from  $0^\circ$  (blue color), to  $90^\circ$  (red color). For both cases, the regions with  $\chi_r \simeq 0$  are nearly aligned with the direction of the unperturbed magnetic field as imposed in each model. This ‘radial’ region is tilted clockwise  $\sim 30^\circ$  respect to the  $\hat{y}$  or ‘North’ direction (see panels (b) of Figure 4) for the quasi-perpendicular case, and  $\sim 60^\circ$  counterclockwise for the quasi-parallel case (see panel (a) of Figure 4). The quasi-parallel model gives a very good agreement (at large scales) with the observations (see Figures 7(a) and (b) in Reynoso et al. 2013), suggesting that the direction of the ambient magnetic field proposed in this model must be representative of the actual orientation. We must note however, that the polar-referenced angles show some spread at small scales. This is most likely due to inhomogeneities of the magnetic field at such scales, which is not accounted for in our simulations.

## 5 DISCUSSION AND CONCLUSIONS

We have utilized 3D MHD models to simulate the polarized emission of SN 1006. The 3D simulations allow us to explore configurations that were impossible with the axisymmetric code used in Schneider et al. (2010). In particular it is possible to test different orientations of the magnetic field with respect to the plane of the sky and avoids some artifacts that arise when generating synthetic maps.

SN 1006 is a member of a population of ‘barrel-like’ or ‘bilateral’ SNRs. Previous studies (Reynolds & Gilmore 1993; Petruk et al. 2009; Schneider et al. 2010; Bocchino et al. 2011; Reynoso et al. 2013) have shown that the emission geometry of bilateral SNRs is correlated with the orientation of the ambient interstellar magnetic field. Different orientations of the magnetic field can be inferred depending upon which particle acceleration mechanism is assumed to be taking place at the SNR shock front, either the quasi-parallel or the quasi-perpendicular model.

As mentioned above, there is an ongoing debate as to which of these two particle acceleration mechanisms is responsible for the observed synchrotron emission in SNRs. While observational works seem to support the quasi-parallel model (polar cap scenario), theoretical studies are not conclusive. A probable reason for this discrepancy is that most of the theoretical works base their conclusions on criteria which only take into account the brightness distribution of the synchrotron emission.

In the present work, we explore if a theoretical polar-

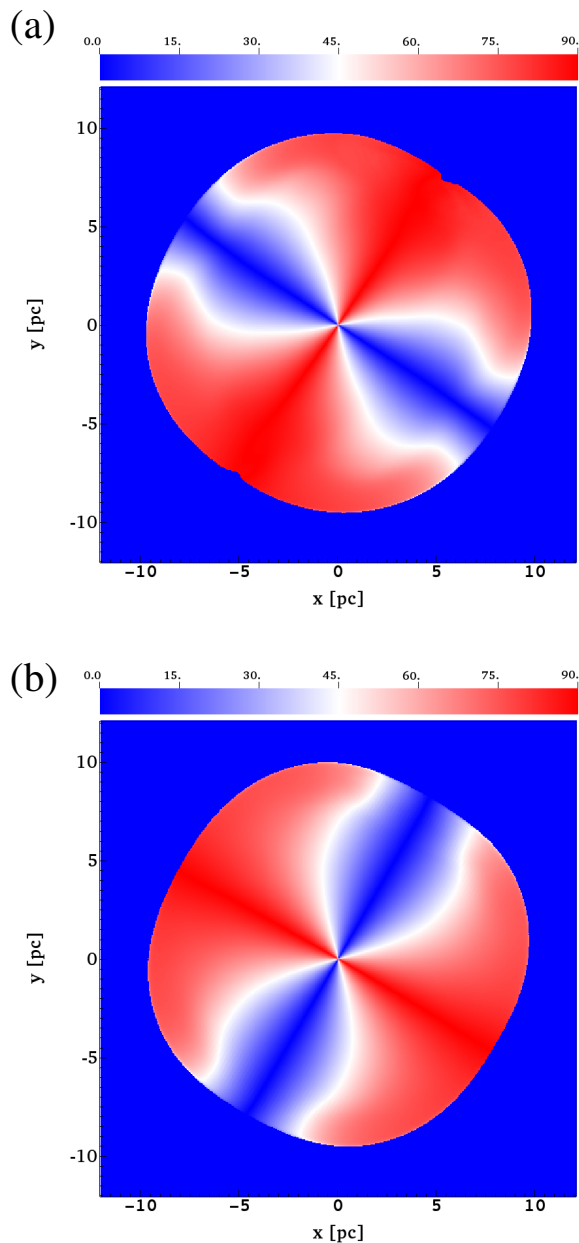


**Figure 4.** Synthetic polar-referenced angle maps obtained for the quasi-parallel (panel a) and quasi-perpendicular (panel b) cases. These maps were rotated 60 degrees with the purpose of comparing them to the observations. The axes are in pc and the linear color scale is given in degrees.

ization study can be a useful tool to shed some light on this question. We synthesized maps of the polarized emission that include Stokes  $Q$  and  $U$ , and the distribution of the polar-referenced angle  $\chi_r$ . In our analysis, we considered two scenarios: (1) an equatorial belt model where the bright rims of SN 1006 are formed from particle acceleration that occurs when the shock passes through interstellar magnetic fields that are perpendicular to the shock normal (quasi-perpendicular); (2) a polar cap model where the bright rims are formed from acceleration that occurs when the shock

passes through magnetic fields that are parallel to the shock normal (quasi-parallel).

The resulting polarized intensity maps alone are not sufficient to decide which mechanism is the adequate to explain the radio morphology of SN 1006 since both scenarios, quasi-parallel and quasi-perpendicular, yield similar results. On the contrary, the synthetic  $Q$  maps for the quasi-parallel and quasi-perpendicular cases differ much from each other. The quasi-perpendicular  $Q$  map displays regions with negative values resembling the bright rims observed in the polarized intensity maps. This result is in disagreement with the observations, which mainly display positive values (Fig. 3; see also Reynolds & Gilmore 1993). In addition, our simulated  $Q$  map for the quasi-parallel case coincides with observations in that the maxima are spatially coincident with the bright arcs of SN 1006, as obtained in our synthetic  $Q$  map for the quasi-parallel case. Finally, the synthetic polar-referenced angle map for the quasi-parallel model is in very good agreement with the results reported by Reynoso et al. (2013).

Our results agree with Bocchino et al. (2011) in that the ISM magnetic field must be parallel to the galactic plane, tilted with respect to the  $los$ , and with a gradient that explains the asymmetry in the emission between the arcs. The difference between their result and ours lies in the degree of inclination with respect to the  $los$ . For the parameter  $Q$  to be comparable to the observations, we employed an inclination of  $75^\circ$  with respect to the  $los$  ( $15^\circ$  respect to the plane of the sky), which is somewhat larger than the best fit ( $38^\circ \pm 4^\circ$ ) reported in Bocchino et al. (2011).

We calculated the polar-referenced angle ( $\chi_r$ ) distribution and found a good agreement with the observations of SN 1006 of Reynoso et al. (2013). The maps of observed  $\chi_r$  show small scale structure that is absent on our models due to the well ordered field imposed. This technique might prove helpful for future studies that include the inhomogeneity of the media or of the magnetic field structure.

In summary, our polarization results provide a strong support to the quasi parallel model, which is in agreement with previous observational (Reynoso et al. 2013) and theoretical works (Bocchino et al. 2011). More importantly, the Stokes parameter  $Q$  proved to be a powerful tool to determine the particle acceleration mechanism that best explains the observed morphology and polarization seen in SN 1006. We note that in a previous 2D MHD numerical simulation, Schneider et al. (2010) concluded that the quasi-perpendicular model was the most suitable to explain the observations. Our paper shows the importance of using 3D simulations, since limiting the analysis to what is possible with an axisymmetric setup led to an opposite result. Only a 3D model can account for a magnetic field that is tilted with respect to the  $los$  and can provide a realistic description of the particle acceleration and synchrotron emission of an SNR.

## ACKNOWLEDGMENTS

We thank the referee for his valuable comments which helped us to improve the original version of the manuscript. EMS and EMR are Member of the Carrera del Investigador Científico, CONICET (Argentina). We acknowledge

Enrique Palacios Boneta for maintaining the Linux server where our simulations were carried out. EMS, PFV, AE, and FDC thank financial support from CONACyT (México) grants 167611 and 167625, CONACyT-CONICET grant CAR 190489 and DGAPA-PAPIIT (UNAM) IG100214, IA101614, 101413, and 103315. EMR is supported by CONICET grant PIP 112-201207-00226.

## REFERENCES

- Acero F., Ballet J., Decourchelle A., 2007, *A&A*, 475, 883  
 Bocchino F., Orlando S., Miceli M., Petruk O., 2011, *A&A*, 531, A129  
 Cassam-Chenaï G., Hughes J. P., Reynoso E. M., Badenes C., Moffett D., 2008, *ApJ*, 680, 1180  
 Clarke D. A., Burns J. O., Norman M. L., 1989, *ApJ*, 342, 700  
 De Colle F., Granot J., López-Cámara D., Ramirez-Ruiz E., 2012, *ApJ*, 746, 122  
 De Colle F., Raga A. C., 2006, *A&A*, 449, 1061  
 De Colle F., Raga A. C., Esquivel A., 2008, *ApJ*, 689, 302  
 Fulbright M. S., Reynolds S. P., 1990, *ApJ*, 357, 591  
 Ginzburg V. L., Syrovatskii S. I., 1965, *ARA&A*, 3, 297  
 Jokipii J. R., 1987, *ApJ*, 313, 842  
 Jun B.-I., Norman M. L., 1996a, *ApJ*, 472, 245  
 Jun B.-I., Norman M. L., 1996b, *ApJ*, 465, 800  
 Orlando S., Bocchino F., Reale F., Peres G., Petruk O., 2007, *A&A*, 470, 927  
 Petruk O., Dubner G., Castelletti G., Bocchino F., Iakubovskiy D., Kirsch M. G. F., Miceli M., Orlando S., Telezhinsky I., 2009, *MNRAS*, 393, 1034  
 Reynolds S. P., Gilmore D. M., 1993, *AJ*, 106, 272  
 Reynoso E. M., Hughes J. P., Moffett D. A., 2013, *AJ*, 145, 104  
 Rothenflug R., Ballet J., Dubner G., Giacani E., Decourchelle A., Ferrando P., 2004, *A&A*, 425, 121  
 Schneider E. M., Velázquez P. F., Reynoso E. M., de Colle F., 2010, *MNRAS*, 408, 430  
 Stephenson F. R., Green D. A., 2002, *Historical supernovae and their remnants*, by F. Richard Stephenson and David A. Green. International series in astronomy and astrophysics, vol. 5. Oxford: Clarendon Press, 2002, ISBN 0198507666, 5  
 Völck H. J., Berezhko E. G., Ksenofontov L. T., 2003, *A&A*, 409, 563  
 Winkler P. F., Gupta G., Long K. S., 2003, *ApJ*, 585, 324